Seizure: European Journal of Epilepsy 111 (2023) 130–137

Contents lists available at ScienceDirect

Seizure: European Journal of Epilepsy

journal homepage: www.elsevier.com/locate/seizure

More extensive structural damage in temporal lobe epilepsy with hippocampal sclerosis type 1

Wei Li [a,b], Yuchao Jiang [c], Xiuli Li [d], Huan Huang [c], Du Lei [d], Jinmei Li [a], Heng Zhang [e], Dezhong Yao [c], Cheng Luo [c], Qiyong Gong [d,1], Dong Zhou [a,1,*], Dongmei An [a,1,*]

[a] Department of Neurology, West China Hospital, Sichuan University, Chengdu, Sichuan, China
[b] National Clinical Research Center for Geriatrics, Department of Gerontology and Geriatrics, West China Hospital, Sichuan University, Chengdu, China
[c] The Clinical Hospital of Chengdu Brain Science Institute, MOE Key Lab for Neuroinformation, Center for Information in Medicine, School of life Science and technology, University of Electronic Science and Technology of China, Chengdu, Sichuan, China
[d] Huaxi MR Research Center, Department of Radiology, West China Hospital, Sichuan University, Chengdu, Sichuan, China
[e] Department of Neurosurgery, West China Hospital, Sichuan University, Chengdu, Sichuan, China

ARTICLE INFO

Keywords:
Mesial temporal lobe epilepsy
Hippocampal sclerosis
Subtype
Structural damage
Connectome

ABSTRACT

Objective: To explore clinical and structural differences between mesial temporal lobe epilepsy (mTLE) patients with different hippocampal sclerosis (HS) subtypes.
Methods: High-resolution T1-weighted MRI and diffusion tensor imaging data were obtained in 41 refractory mTLE patients and 52 age- and sex-matched healthy controls. Postoperative histopathological examination confirmed HS type 1 in 30 patients and HS type 2 in eleven patients. Clinical features, postoperative seizure outcomes, hippocampal subfields volumes, fractional anisotropy (FA) values of white matter regions and graph theory parameters were explored and compared between the HS type 1 and HS type 2 groups.
Results: No significant differences in clinical features and postsurgical seizure outcomes were found between the HS type 1 and type 2 groups. However, the HS type 1 group showed extra atrophy in ipsilateral parasubiculum than healthy controls and more severe atrophy in contralateral hippocampal fissure than the HS type 2 group. More extensive FA decrease were also observed in the HS type 1 group, involving ipsilateral optic radiation, superior fronto-occipital fasciculus, contralateral uncinate fasciculus, tapetum, bilateral hippocampal cingulum, corona radiata, etc. Furthermore, in spite of similar impairments in characteristic path length, global efficiency and local efficiency in two HS groups, the HS type 1 group showed additional decrease of clustering coefficient than healthy controls.
Conclusions: HS type 1 and 2 groups had similar clinical characteristics and postoperative seizure outcomes. More widespread neuronal cell loss in the HS type 1 group contributed to more extensive structural damage and connectivity abnormality. These results shed new light on the imaging correlates of different HS pathology.

1. Introduction

Mesial temporal lobe epilepsy (mTLE) is the most common medically intractable but surgically remediable epilepsy in adults, with a characteristic seizure semiology and unilateral EEG onset [1,2]. The hippocampus is commonly regarded as the seizure focus in mTLE, with widespread cortical and subcortical regions involved [3,4]. As the most established therapeutic procedure for refractory mTLE, anterior temporal lobectomy (ATL) resects the hippocampus and adjacent mesial temporal structures, offering a favorable seizure-freedom rate of 60–70% [5,6]. However, 30–40% of mTLE patients continue to have seizures after surgery, and the proportion will increase as the follow-up time extends [7,8]. To date, the underlying pathological mechanism is not well-known.

Histopathological examinations of postmortem or surgical specimens have revealed hippocampal sclerosis (HS) to be the most frequent histopathology underlying drug-resistant mTLE [9,10]. The main hallmark of HS is neuronal cell loss and chronic gliosis centered on the pyramidal

* Corresponding authors at: Huaxi MR Research Center, Department of Radiology, Center for Medical Imaging, West China Hospital, Sichuan University, Chengdu, Sichuan, China.
E-mail addresses: qiyonggong@hmrrc.org.cn (Q. Gong), zhoudong66@yahoo.de (D. Zhou), dongmeian@scu.edu.cn (D. An).
[1] These authors contributed to this work equally.

https://doi.org/10.1016/j.seizure.2023.08.003
Received 23 March 2023; Received in revised form 4 August 2023; Accepted 6 August 2023
Available online 7 August 2023

cell layer [2]. The latest classification of International League Against Epilepsy (ILAE) [9] divided HS into three subtypes: HS type 1 (accounting for 60–80%) refers to severe neuronal cell loss and gliosis predominantly in region 1 and 4 of cornu ammonis (CA), while HS type 2 and type 3 refer to predominant neuronal cell loss and gliosis in CA1 and CA4 respectively. Reactive gliosis alone without neuronal cell loss (known as no-HS) occurs in some patients. It was thought that different histopathological subtypes of HS may reflect distinct pathological mechanisms of mTLE, leading to different clinical and neuroimaging features [11–20]. However, the association of clinical, neuroimaging and pathological characteristics with different HS types has not been systematically studied.

Some clinical observations pointed to different clinical features and seizure outcome of HS subtypes. Compared to typical HS (HS type 1), atypical HS (including HS type 2, 3 and no-HS) was thought to have a later age of initial precipitating injury [11], a later age of habitual seizure onset [12,13] and less common history of febrile seizures [11]. Furthermore, atypical HS was thought to be related to worse postsurgical seizure outcomes [11–13]. However, these results were not consistently discovered, and few studies revealed direct comparisons between different HS subtypes based on recent histopathological classifications [9]. One clinical study including patients with HS type 1, 2, 3 and gliosis/no-HS found no differences in the duration of epilepsy, onset age of epilepsy, side of HS, history of febrile seizures and EEG findings. However, compared with patients with HS type 1, patients with HS types 2 and 3 had a more frequent history of secondarily generalized tonic-clonic seizure (sGTCS) and a family history of epilepsy [14]. Another study enrolling three HS subtypes and coexisted focal cortical dysplasia (FCD) indicated that HS subtypes shared similar demographic and etiologic characteristics and postoperative seizure outcomes [15].

Although routine MRI provides some evidence of HS, including hippocampal atrophy, hyperintensity on T2-weighted imaging and disturbed internal architecture of the hippocampus, it is difficult to visually differentiate HS subtypes from preoperative imaging. There is an urgent need to develop sensitive neuroimaging techniques to characterize hippocampal pathology in mTLE patients presurgically, which may influence surgery planning. With the help of emerging neuroimaging techniques, some evidence indicated higher resolution (4.0/4.7/7.0 T) MRI could help to parcellate hippocampal subfields and determine HS subtype preoperatively [16–18]. However, these methods have not been regularly used in clinical assessment. Recent multimodal MRI studies using 3.0T MRI revealed structural and functional differences between TLE patients with HS and gliosis only (no-HS), indicating HS modulated more marked effects on large-scale brain networks [19,20]. However, there is limited understanding of whether more extensive HS pathology (HS type 1 > HS type 2 > HS type 3) led to more serious damage to structural networks.

Previous studies provided some clinical and neuroimaging differences between distinct HS subtypes, mainly between typical and atypical HS, or between typical HS and no-HS type. There was little evidence of direct comparisons between these two main HS subtypes: HS type 1 and HS type 2. Furthermore, little attention was paid to differences in white matters or structural connectomes. In this study, we explored clinical features, postoperative seizure outcomes, hippocampal subfields volumes, fractional anisotropy (FA) of white matters and structural connectomes in mTLE patients with definite HS pathology (HS type 1 and HS type 2). We expected to reveal direct differences in neuroimaging and clinical features between HS type 1 and HS type 2 using the most commonly used 3.0T MRI, which may contribute to differentiating these two HS subtypes before surgery and predict postsurgical seizure outcomes. In addition, these results may shed lights on the imaging correlates of HS and provide new insight into the pathological mechanisms of HS-associated mTLE.

2. Materials and methods

2.1. Participants

We consecutively included refractory mTLE patients who aimed to receive resective surgery at West China Hospital from December 2014 to March 2019. The mTLE diagnosis was made according to the ILAE classification criteria [21]. All patients underwent comprehensive presurgical evaluations of clinical symptoms, ictal and interictal EEG, brain MRI and possible positron emission tomography (PET) to localize the seizure focus. High-resolution T1-weighted structural MRI and diffusion tensor imaging (DTI) data were also acquired before surgery. All patients underwent resective surgery and histopathological examination at West China Hospital. Postoperative seizure outcomes were assessed by two investigators without knowing the pathological results at 24 months after surgery according to the ILAE classification [5].

Our inclusion criteria were as follows: (1) patients were diagnosed as intractable mTLE according to the ILAE criteria; (2) patients with normal MRI or with unilateral HS evidence in keeping with EEG findings; (3) patients were suitable for resective surgery after a multidisciplinary presurgical assessment; (4) HS was confirmed and classified by postsurgical histopathological examination according to the ILAE classification [9].

Our exclusion criteria were as follows: (1) patients with other neurological, psychiatric, or severe systemic disorders; (2) patients with alcohol or other substances abuse; (3) patients with bilateral HS or other structural lesions; (4) resected hippocampal tissue was not enough to conduct the HS classification.

In the end, two patients with FCD, one patient with obvious extratemporal atrophy, twelve patients without enough hippocampal tissue for pathological classification were excluded. Definite histopathological classifications were confirmed in 45 patients, including 30 patients with HS type 1, eleven patients with HS type 2, one patient with HS type 3, and three patients with gliosis only (no-HS). Considering the small number of HS type 3 and no-HS group, we only enrolled HS type 1 and HS type 2 group for further analysis. Besides, 3D-T1 and DTI data were also acquired with the same protocol in age- and sex-matched healthy controls (HC) without any neurological or psychiatric disorders.

This study was approved by the local ethics committee of West China Hospital and informed consent was obtained from all subjects.

2.2. Image acquisition

We obtained all MRI data on a 3.0 T MRI system (Siemens, Erlangen, Germany) at West China Hospital. We applied a 3D magnetization-prepared rapid gradient-echo (MPRAGE) sequence to acquire T1-weighted structural images as our previous study [22]. The T1 images are widely used to detect structural abnormalities in the brain, which enable quantitative assessment of the volume of brain tissue and individual brain structures. Detailed parameters were as follows: repetition time (TR) = 1900 ms; echo time (TE) = 2.26 ms; flip angle = 9°; slice thickness = 1 mm; field of view (FOV) = 256 × 256 mm^2; voxel size = 1.0 × 1.0 × 1.0 mm^3. We also applied a spin-echo planar imaging sequence to acquire the DTI data. DTI provides an indirect method of assessing neuroanatomy structure on a microscopic level using water molecules' degree of anisotropy and structural orientation within a voxel. Detailed parameters were as follows: TR = 6800 ms; TE = 91 ms; matrix = 256 × 256; FOV = 240 × 240 mm^2; slice thickness = 3 mm, no gap, 50 slices. Diffusion weighting was encoded along 64 non-collinear directions (b = 1000s/mm^2) and no diffusion weighting (b0 image) was used as the reference image. During the whole scanning, participants were instructed to keep their heads still and relax with their eyes closed. We used an eight-channel birdcage head coil and a restraining foam pad to minimize the head motion, as well as earplugs to reduce the noise and improve the comfort.

2.3. Image processing

Before processing, all 3D-TI and DTI images were visually checked. Any images with obvious blurring/ringing/ghosting or other artefacts were ruled out. Freesurfer [23] (version 6.0, http://surfer.nmr.mgh.harvard.edu/) was applied to segment the hippocampus and measure the volumes of hippocampal subfields, which was proved to have a good accordance with HS histology [24]. The processing steps of T1 images included skull stripping, tissue segmentation, surface reconstruction, registration and parcellation. Specifically, we use the recon-all command, a full processing stream for structural MRI data, including the segment of hippocampus and measure the volumes of hippocampal subfields (https://surfer.nmr.mgh.harvard.edu/fswiki/HippocampalSubfields). The hippocampus in each hemisphere was divided into 12 subfields, including the hippocampal tail, subiculum, CA1, hippocampal fissure, presubiculum, parasubiculum, molecular layer of the hippocampus, granular cells layer of the dentate gyrus (GC-DG), CA3, CA4, fimbria and hippocampus-amygdala transition area (HATA). The volumes of all hippocampal subfields and the whole hippocampus were calculated for each hemisphere. All segmentation results were visually verified to ensure image quality.

Similar to the processing applied in the ENIGMA project (http://enigma.ini.usc.edu/protocols/dti-protocols) and our previous study [25], the FSL software (version 6.0) [26] and Tract-Based Spatial Statistics (TBSS) [27] were applied to process the DTI data. There are a number of measures calculated using DTI that can provide quantitative power. One of the most widely used DTI measures is fractional anisotropy (FA). Others include mean diffusivity or apparent diffusion coefficient (ADC), radial (perpendicular) diffusivity, and axial (parallel) diffusivity. In this study, the FA was used to evaluate the neurostructural abnormalities of the patients. Specifically, by preprocessing, raw DICOM images were converted to FA images for each subject and quality control was performed along the way to remove scans with abnormalities and artifacts (https://enigma.ini.usc.edu/wp-content/uploads/DTI_Protocols/ENIGMA_FA_V1_QC_protocol_USC.pdf). The DTI FA image is then fed into TBSS, which aligns the FA image onto a standard-space white-matter skeleton, with alignment improved over the original TBSS skeleton-projection methodology through a high-dimensional FNIRT--based warping. The resulting standard-space warp (TBSS/FA/dti_FA_to_MNI_warp) is applied to all other DTI/NODDI outputs. The final skeleton-space outputs are in TBSS/stats/all_*_skeletonised, where * represents each of the DTI and NODDI outputs (FA, etc.). For each of the DTI/NODDI outputs, these skeletonised images are averaged across a set of 48 standard-space tract masks defined by the group of Susumi Mori at Johns Hopkins University [28].

In addition, we also characterized the brain topology of white matter connectivity based on DTI tractography using the graph theory approach. Similar to our previous study [29], white matter structural network analysis was performed and briefly described here. First, diffusion tensor imaging tractography was used to map the whole brain white matter structural network, composed of 90 cortical and sub-cortical regions based on the Automated Anatomical Labeling (AAL) atlas [30]. Second, graph theoretical methods were applied to investigate the alterations in the topological properties of the networks in these patients. Brain Connectivity Toolbox (BCT) [31] was applied to calculate graph theory metrics, including the clustering coefficient, characteristic path length, global and local efficiency.

2.4. Statistical analysis

Statistical analyses were performed using SPSS (version 22.0). Categorical demographic and clinical variables were analyzed using the chi-square test or Fisher's exact test, while continuous variables were analyzed using two-sample *t*-test. After calculating the volume of individual's hippocampal subregion, an analysis of covariate (ANCOVA) was used to detect differences of hippocampal subfield volumes among three groups (HS type 1 vs. HS type 2 vs. HC), with age, gender and intracranial volumes (ICV) as covariates. Then, the two-sample *t*-test was used to compare the volume differences between any two of the three groups. $P < 0.05$ was considered as statistical significance. Similarly, ANCOVA with age and gender as covariates and post-hoc t-tests were applied to find differences in FA values and graph theory metrics among the three groups. False discovery rate (FDR) correction was applied for multiple comparisons. An FDR-corrected *P*value < 0.05 was considered statistically significant.

2.5. Availability of data

Anonymized data will be available upon request for qualified investigators.

3. Results

3.1. Participants

Finally, forty-one mTLE-HS patients (24 males) were enrolled in the analysis. They had a median age at surgery of 25.9 years old and a median duration of epilepsy of 12 years. All patients had at least one seizure per month before surgery, with or without focal to bilateral tonic-clonic seizure (FBTCS). All patients underwent standard ATL (L/R, 21/20) by one experiential neurosurgeon. HS was pathologically confirmed in all patients, including 30 patients with HS type 1 and 11 patients with HS type 2. The postsurgical seizure outcomes were assessed at 24 months after surgery. Furthermore, 52 healthy controls (31 males), with a mean age of 26.8 years old were included. All participants were native Chinese speakers and were scanned with the same protocol. All subjects were right-handed except one patient was forced right-handed.

There was no statistically significant difference in gender and age among the three groups (HS type 1 vs. HS type 2 vs. HC) and between HS type 1 and type 2 group. In additions, there was no obvious difference between the HS type 1 and type 2 group in many clinical features, including seizure duration, history of brain injury, history of febrile seizure, seizure type, seizure frequency, side of HS, HS evidence from MRI and postsurgical seizure-free rate ($P > 0.05$). Detailed clinical and demographic information of all subjects were summarized in Table 1.

3.2. Hippocampal subfields volumes

At the whole hippocampus level, both HS type 1 and type 2 groups showed significantly smaller volume than HC in the ipsilateral hippocampus ($P < 0.005$), without obvious volume difference between the HS type 1 and type 2 groups. There were also no obvious differences in contralateral hippocampus volume among patients and controls.

At the hippocampal subfields level, significant volume differences were observed in ipsilateral hippocampal tail, subiculum, CA1, presubiculum, parasubiculum, molecular layer, GC-DG, CA3, CA4, fimbria, HATA, as well as contralateral hippocampal fissure among three groups ($P < 0.005$).

Within these hippocampal subfields with obvious volume differences, (1) HS type 1 and type 2 group showed consistently smaller volumes than HC in the ipsilateral hippocampal tail, subiculum, CA1, presubiculum, molecular layer, GC-DG, CA3, CA4, fimbria, and HATA (Fig. 1A); (2) only HS type 1 group showed significantly smaller volume than HC in ipsilateral parasubiculum ($P < 0.005$) (Fig. 1B); (3) HS type 1 group showed significantly smaller volume than HS type 2 group in contralateral hippocampal fissure ($P < 0.005$) (Fig. 1C).

3.3. FA values of different white matter regions

Comparing among three groups (HS type 1 vs. HS type 2 vs. HC), significant FA differences were observed in ipsilateral medial lemniscus

Table 1
Clinical and demographic characteristics of the subjects.

	HS type 1 (n = 30)	HS type 2 (n = 11)	HC (n = 52)	F/χ^2	P value
Gender (male/female)	18/12	6/5	31/21	0.110 [a]	0.946 [a]
				0.099 [b]	0.753 [b]
Age (year)					
mean ± SD (range)	26.7 ± 8.6 (17–47)	23.5 ± 8.2 (15–42)	26.8 ± 6.8 (16–49)	0.898 [a]	0.411 [a]
				0.490 [b]	0.488 [b]
Seizure duration (year)					
mean ± SD (range)	12.3 ± 9.4 (2–46)	11.6 ± 8.1 (1–23)	–	0.000	0.984
History of brain injury	6 (20.0%)	2 (18.2%)	–	0.017	0.896
History of febrile seizure	13 (43.3%)	5 (45.5%)	–	0.015	0.903
Seizure type					
FS/FS+FBTCS	11/19	3/8	–	0.316	0.574
Seizure frequency					
daily/weekly/monthly	3/16/11	0/5/6	–	1.818	0.403
Side of HS (L/R)	13/17	8/3	–	2.783	0.095
HS evidence from MRI	28 (90.0%)	9 (81.8%)		0.503	0.478
Postsurgical seizure freedom	23 (76.6%)	8 (72.7%)		0.068	0.795

Abbreviations: HS = hippocampal sclerosis; HC = healthy controls; SD = standard deviation; FS = focal seizure; FBTCS = focal to bilateral tonic-clonic seizure; L = left; R = right. [a] comparison among the three groups; [b] comparison between the HS type 1 and type 2 groups.

(ML), superior cerebellar peduncle (sCBLP), cerebral peduncle (CBRP), anterior limb of internal capsule (ALIC), anterior corona radiata (ACR), superior corona radiata (SCR), posterior corona radiata (PCR), optic radiation (OR), sagittal stratum (SS), external capsule (EC), cingulum (cingulate gyrus) (CGG), cingulum (hippocampus) (CGH), fornix (cres) (FXC), superior longitudinal fasciculus (SLF), superior frontal-occipital fasciculus (SFO), uncinate fasciculus (UF); contralateral ML, sCBLP, ACR, SCR, PCR, OR, EC, CGH, SLF, UF, tapetum (TAP); as well as middle cerebellar peduncle (mCBLP), genu of corpus callosum (GCC), body of corpus callosum (BCC), fornix (FX). Detailed white matter regions with obvious FA changes are shown in Fig. 2.

Within those white matter regions with obvious FA differences, (1) HS type 1 and 2 group showed consistently smaller FA than HC in ipsilateral sCBLP, ALIC, ACR, SCR, EC, CGG, FXC, SLF, UF, contralateral ACR, PCR, OR, EC, SLF, as well as GCC, BCC, FX (Fig. 3A); (2) only HS type 1 group showed significantly smaller FA than HC in ipsilateral CBRP, PCR, OR, SS, CGH, SFO, contralateral ML, sCBLP, SCR, CGH, UF, TAP, as well as mCBLP (Fig. 3B); (3) only HS type 2 group showed significantly smaller FA than HC in ipsilateral ML (Fig. 3C).

3.4. Graph-theoretic parameters

Figure 4 shows significant differences in clustering coefficient, characteristic path length, global efficiency and local efficiency among three groups (HS type 1 vs. HS type 2 vs. HC).

Within them, (1) the HS type 1 and HS type 2 groups showed consistently higher characteristic path length, lower global efficiency and local efficiency than HC; (2) only the HS type 1 group showed a significantly lower clustering coefficient than HC.

4. Discussion

This present study explored potential clinical and structural differences in mTLE patients with the two most common HS types (HS type 1 and HS type 2). We noted no significant differences in demographic and clinical features or seizure outcomes after resective surgery. However, we found more widespread structural abnormalities in mTLE patients with HS type 1 than those with HS type 2, including more obvious hippocampal subfields atrophy, more extensive diffusion abnormality, and severe structural connectome impairment. These results reflected more widespread neuronal cell loss and gliosis (involving CA 1 and CA 4 rather than CA 1 only) contributed to more extensive structural damage and connectivity abnormality. To our knowledge, this was the first study to directly compare the clinical and neuroimaging differences between patients with HS type 1 and type 2. It provided direct evidence of the consistency of pathological changes and neuroimaging abnormalities and shed new light on the imaging correlates of different HS pathology.

Previous studies revealed some different clinical features between

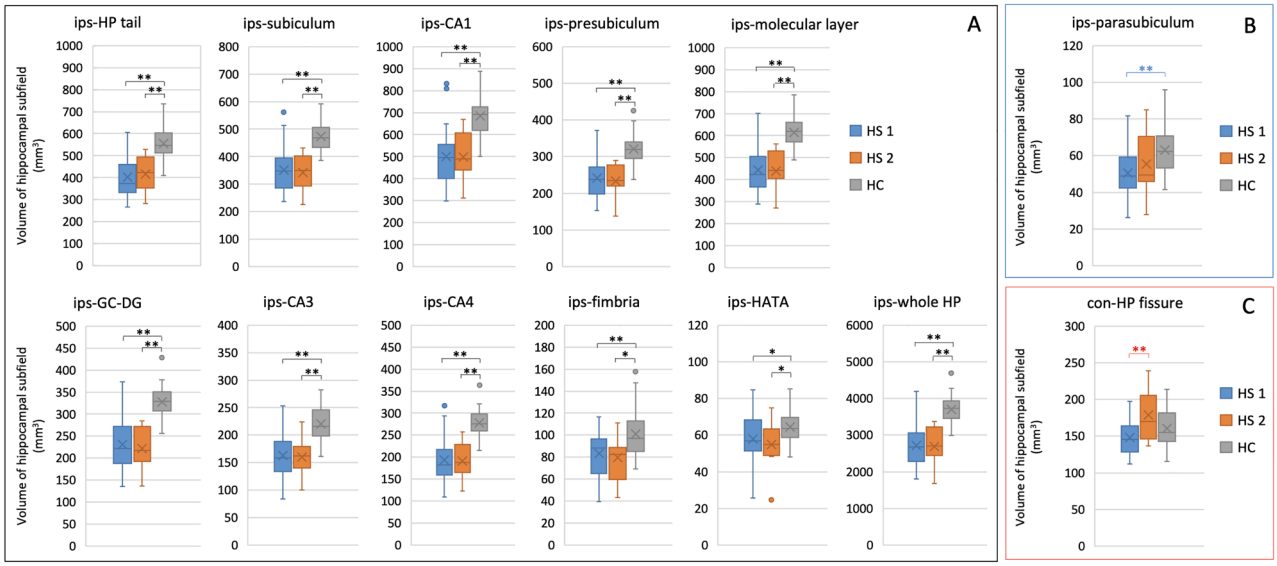

Fig. 1. Comparisons of hippocampal subfields volumes among patients and controls. Abbreviations: HS 1 = hippocampus sclerosis type 1; HS 2 = hippocampus sclerosis type 2; HC = healthy controls; HP = hippocampus; CA = cornu ammonis; GC-DG = granular cells layer of the dentate gyrus; HATA = hippocampus-amygdala transition area. ** $P < 0.005$, * $P < 0.05$.

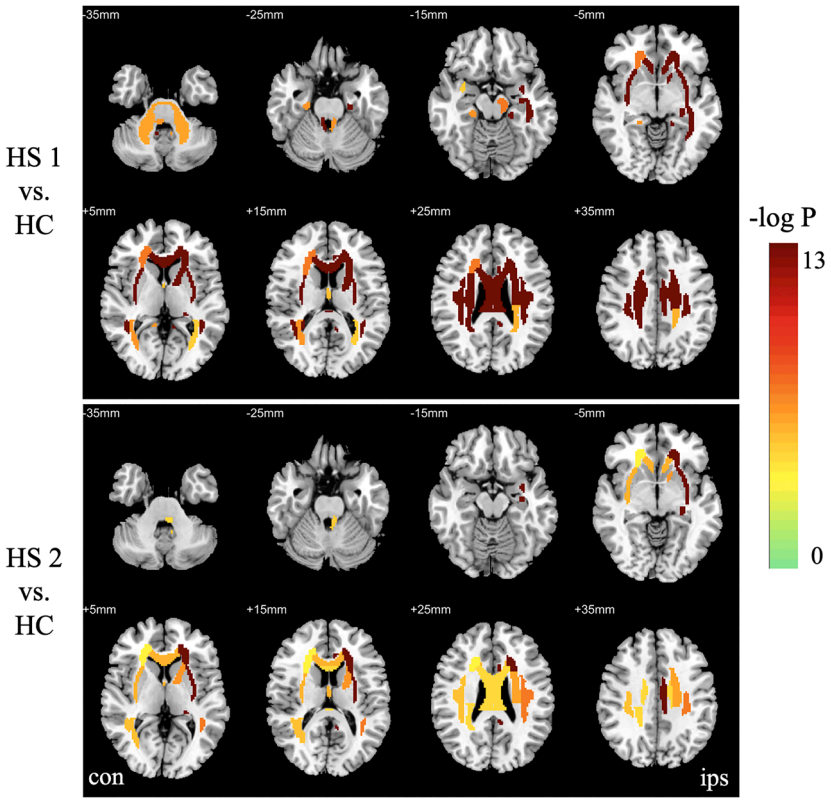

Fig. 2. White matter regions with significant FA changes in HS subtypes. Abbreviations: HS 1 = hippocampus sclerosis type 1; HS 2 = hippocampus sclerosis type 2; HC = healthy controls; con = contralateral hemisphere; ips = ipsilateral hemisphere.

HS subtypes, including age of initial precipitating injury, age of seizure onset, history of febrile seizures, family history of epilepsy, history of sGTCS and postsurgical seizure outcome [11–14]. However, these results were not consistently discovered, which might result from different histopathological classifications and different combinations of HS subtypes (typical HS vs. atypical HS; HS type 1 vs. HS type 2&3; typical HS vs. no-HS). In this present study, we only recruited patients with the two most common HS types (HS type 1 and HS type 2) based on the latest ILAE classification [9]. We found no obvious differences in clinical and demographic characteristics between patients with HS type 1 and type 2. Furthermore, although it seemed that the postsurgical seizure-free rate was relatively higher in the HS type 1 group (76.6%) than in the HS type 2 group (72.7%), the difference was not statistically significant (P = 0.795). There was a possibility that previously discovered clinical differences were mostly due to differences between HS type 1 and the no-HS group. The heterogeneity between HS type 1 and HS type 2 was indeed not as big as we used to think. These speculations were supported by previous findings from Cleveland Clinic including 307 HS patients that HS subtypes shared similar demographic and etiologic characteristics, as well as postoperative seizure outcomes [15].

Regarding the volume of hippocampal subfields, both HS type 1 and HS type 2 groups showed significant atrophy in the ipsilateral hippocampal tail, subiculum, CA1, presubiculum, molecular layer, GC-DG, CA3, CA4, fimbria and HATA. A similar high effect of atrophy in HS type 1 and HS type 2 was also observed before [19]. It was interesting that volume decrease in ipsilateral CA4 was consistently observed in two groups, although neuronal cell loss was not severe in CA4 in the HS type 2 group. It was probable that mild neuronal cell loss also caused obvious volume change which could be detected by high-resolution MRI and postprocessing approach. We may need more sensitive neuroimaging techniques and markers to characterize subtle architectural differences. Moreover, we did find some structural differences between the HS type 1 and type 2 groups. Firstly, only the HS type 1 group showed significant atrophy in the ipsilateral parasubiculum than HC. The parasubiculum is located between the presubiculum and the medial entorhinal area and was thought to be involved in spatial information processing [32,33]. Previous studies found neuron loss of parasubiculum in rats with evoked status epilepticus [34,35]. However, the parasubiculum was also not participating in seizure activity propagations in animal TLE models [36]. Up to now, the role of parasubiculum in TLE was not well recognized. Our result provided a preliminary clue that different HS pathology may induce different structural alterations in the parasubiculum. In addition, there was an obvious volume difference in the contralateral hippocampal fissure between the HS type 1 and type 2 groups, indicating different structural influences on the contralateral hippocampus.

Regarding the white matters, both HS type 1 and HS type 2 groups showed marked FA decrease in diffuse white matter regions in the bilateral hemisphere. This was in line with our previous study exploring longitudinal white matter changes before and after mTLE surgery, [25] suggesting diffusion dysfunction induced by uncontrolled seizures and chronic structural changes [37]. Furthermore, we found extra FA decrease in the HS type 1 group, involving ipsilateral optic radiation, superior fronto-occipital fasciculus, contralateral uncinate fasciculus, tapetum, bilateral cingulum (hippocampus), corona radiata, etc. These findings indicated severer and wider neuronal cell loss in the hippocampus led to more extensive diffusion abnormalities in white matter directly or indirectly connected to the hippocampus. Besides, only the HS type 2 group showed reduced FA than HC in the ipsilateral medial lemniscus. Since the medial lemniscus conveyed sensory information to the ipsilateral thalamus directly, [38] reduced FA of the medial lemniscus may reflect specific thalamic dysfunction in the HS type 2 group, which may need further study to confirm.

The graph theoretical approach provides a coherent model to explore the structural connectome in TLE and allows for detecting brain topology changes from both global and regional network perspectives [39]. It is an excellent method to understand structural network alterations

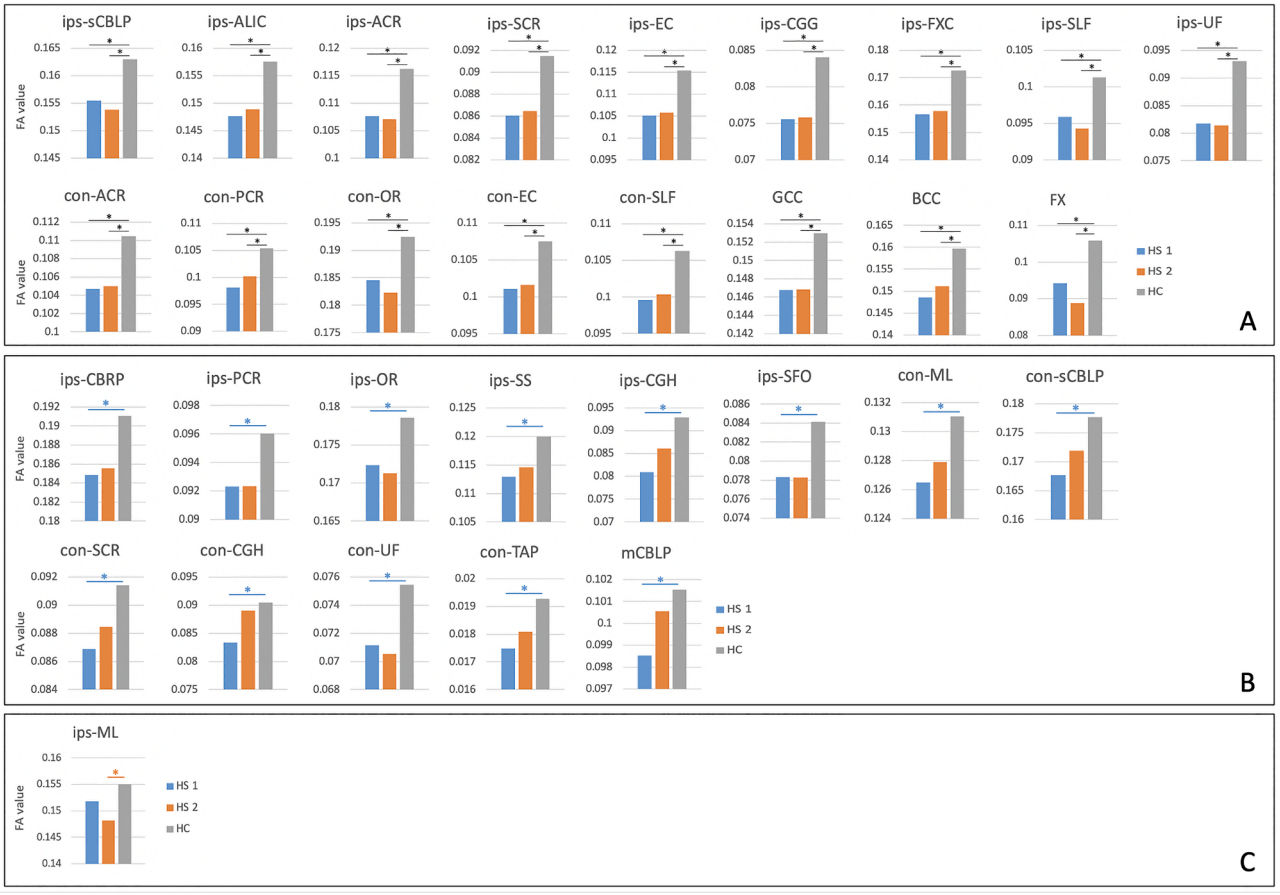

Fig. 3. Comparisons of FA values among patients and controls. Abbreviations: FA = fractional anisotropy; HS 1 = hippocampus sclerosis type 1; HS 2 = hippocampus sclerosis type 2; HC = healthy controls; ips = ipsilateral; con = contralateral; sCBLP = superior cerebellar peduncle; ALIC = anterior limb of internal capsule; ACR = anterior corona radiata; SCR = superior corona radiata; EC = external capsule; CGG = cingulum (cingulate gyrus); FXC = fornix (cres); SLF = superior longitudinal fasciculus; UF = uncinate fasciculus; PCR = posterior corona radiata; OR = optic radiation; GCC = genu of corpus callosum; BCC = body of corpus callosum; FX = fornix; CBRP = cerebral peduncle; SS = sagittal stratum; CGH = cingulum (hippocampus); SFO = superior fronto-occipital fasciculus; ML = medial lemniscus; TAP = tapetum; mCBLP = middle cerebellar peduncle. * $P < 0.05$.

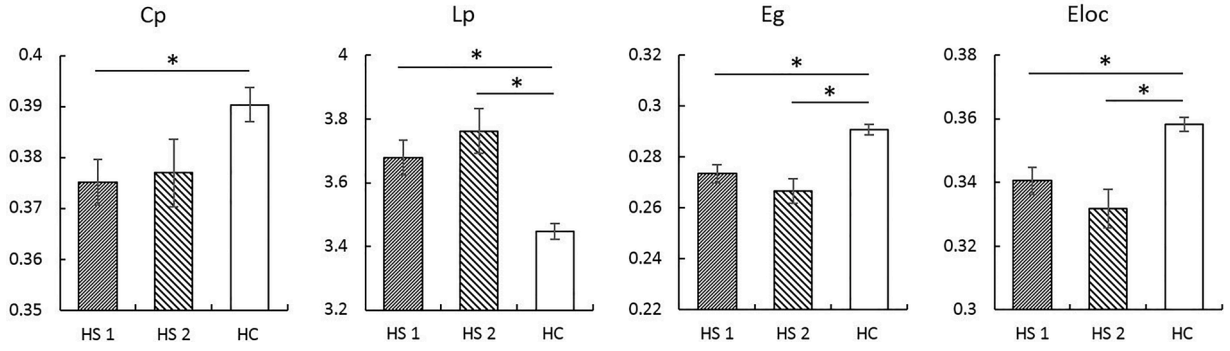

Fig. 4. Comparisons of graph-theoretic parameters among patients and controls. Abbreviations: HS 1 = hippocampus sclerosis type 1; HS 2 = hippocampus sclerosis type 2; HC = healthy controls; Cp = clustering coefficient; Lp = characteristic path length; Eg = global efficiency; Eloc = local efficiency. * $P < 0.05$.

induced by different neuron level changes. Global efficiency is a measure of a network's ability for parallel information transfer while local efficiency is a measure of the efficiency of a given node in communicating with the rest of the brain [39]. Our results suggested HS type 1 and type 2 groups had similar global and local efficiency impairments. However, the HS type 1 group showed markedly increased characteristic path length and decreased clustering coefficient compared to controls, while the HS type 2 group showed smaller effects, only significant for characteristic path length. The characteristic path length is a measure of global connectivity and an index of network integration, reflecting the ability of the network for serial information transfer. Increased characteristic path length indicated decreased level of global network integration [20,39]. While the clustering coefficient is a measure of local connectivity and an index of network segregation, reflecting the local cliquishness of the network [39,40]. Our findings suggested that the HS type 1 and type 2 groups had similar impairments in global connectivity. In contrast, the HS type 1 group had more obvious impairments in local connectivity, which was in keeping with more obvious neuronal cell loss

in the HS type 1 group and provided direct evidence of the correlation between neuroimaging and pathological features. Increased characteristic path length and decreased clustering coefficient were also found in TLE patients before based on diffusion tractography and graph theory, [41] which was in line with our findings in the HS type 1 group. Furthermore, lower clustering coefficient and longer characteristic path length were observed in TLE patients with HS compared to those with gliosis only (no-HS), suggesting severe HS was associated with marked remodeling of connectome topology [20]. Our results further confirmed this and reflected structural connectome differences in patients with and without HS and patients with different HS subtypes, which may be the structural foundation for different seizure outcomes.

4.1. Limitations

A limitation of this study was the small sample size, which may not have sufficient power to address all potential differences. Further studies enrolling more HS patients, especially patients with HS type 2 and type 3, are needed to provide more details. Secondly, we right-left flipped 3D-T1 and DTI images of right-sided mTLE to combine analysis. This procedure ignored potential structural differences in the left and right hemispheres. Further study with more patients was needed to analyze each hemisphere independently.

5. Conclusion

HS type 1 and 2 groups had similar clinical characteristics and postoperative seizure outcomes. More widespread neuronal cell loss in the HS type 1 group contributed to more extensive structural damage and connectivity abnormality. These results shed new light on the imaging correlates of different HS pathology.

Funding

This study was supported by National Natural Science Foundation of China (82171443, 82202242), China Postdoctoral Science Foundation (2022M712251, BX2021078, 2021M700852), Natural Science Foundation of Sichuan Province (2022NSFSC1483), Post-Doctor Research Project, West China Hospital, Sichuan University (2021HXBH062), and Shanghai Sailing Program from Shanghai Science and Technology Committee (22YF1402800).

Declaration of Competing Interest

All authors have no conflicts of interest to declare.

References

[1] Kwan P, Schachter SC, Brodie MJ. Drug-resistant epilepsy. N Engl J Med 2011;365(10):919–26.
[2] Malmgren K, Thom M. Hippocampal sclerosis–origins and imaging. Epilepsia 2012;53(4):19–33. Suppl.
[3] SH Jin, Jeong W, Chung CK. Mesial temporal lobe epilepsy with hippocampal sclerosis is a network disorder with altered cortical hubs. Epilepsia 2015;56(5):772–9.
[4] Mueller SG, Laxer KD, Barakos J, Cheong I, Finlay D, Garcia P, et al. Involvement of the thalamocortical network in TLE with and without mesiotemporal sclerosis. Epilepsia 2010;51(8):1436–45.
[5] Wieser HG, Blume WT, Fish D, Goldensohn E, Hufnagel A, King D, et al. ILAE Commission Report. Proposal for a new classification of outcome with respect to epileptic seizures following epilepsy surgery. Epilepsia 2001;42(2):282–6.
[6] Doherty C, Nowacki AS, Pat McAndrews M, McDonald CR, Reyes A, Kim MS, et al. Predicting mood decline following temporal lobe epilepsy surgery in adults. Epilepsia 2021;62(2):450–9.
[7] de Tisi J, Bell GS, Peacock JL, McEvoy AW, Harkness WF, Sander JW, et al. The long-term outcome of adult epilepsy surgery, patterns of seizure remission, and relapse: a cohort study. Lancet 2011;378(9800):1388–95.
[8] Mohan M, Keller S, Nicolson A, Biswas S, Smith D, Osman Farah J, et al. The long-term outcomes of epilepsy surgery. PLoS ONE 2018;13(5):e0196274.
[9] Blümcke I, Thom M, Aronica E, Armstrong DD, Bartolomei F, Bernasconi A, et al. International consensus classification of hippocampal sclerosis in temporal lobe epilepsy: a Task Force report from the ILAE Commission on Diagnostic Methods. Epilepsia 2013;54(7):1315–29.
[10] Thom M. Review: hippocampal sclerosis in epilepsy: a neuropathology review. Neuropathol Appl Neurobiol 2014;40(5):520–43.
[11] Blümcke I, Pauli E, Clusmann H, Schramm J, Becker A, Elger C, et al. A new clinico-pathological classification system for mesial temporal sclerosis. Acta Neuropathol 2007;113(3):235–44.
[12] de Lanerolle NC, Kim JH, Williamson A, Spencer SS, Zaveri HP, Eid T, et al. A retrospective analysis of hippocampal pathology inhuman temporal lobe epilepsy: evidence for distinctive patient sub-categories. Epilepsia 2003;44(5):677–87.
[13] Thom M, Liagkouras I, Elliot KJ, Martinian L, Harkness W, McEvoy A, et al. Reliability of patterns of hippocampal sclerosis as predictors of postsurgical outcome. Epilepsia 2010;51(9):1801–8.
[14] Tezer FI, Xasiyev F, Soylemezoglu F, Bilginer B, Oguz KK, Saygi S. Clinical and electrophysiological findings in mesial temporal lobe epilepsy with hippocampal sclerosis, based on the recent histopathological classifications. Epilepsy Res 2016;127:50–4.
[15] Gales JM, Jehi L, Nowacki A, Prayson RA. The role of histopathologic subtype in the setting of hippocampal sclerosis-associated mesial temporal lobe epilepsy. Hum Pathol 2017;63:79–88.
[16] Mueller SG, Laxer KD, Barakos J, et al. Subfield atrophy pattern in temporal lobe epilepsy with and without mesial sclerosis detected by high-resolution MRI at 4 Tesla: preliminary results. Epilepsia 2009;50(6):1474–83.
[17] Steve TA, Gargula J, Misaghi E, et al. Hippocampal subfield measurement and ILAE hippocampal sclerosis subtype classification with in vivo 4.7 tesla MRI. Epilepsy Res 2020;161:106279.
[18] Santyr BG, Goubran M, Lau JC, et al. Investigation of hippocampal substructures in focal temporal lobe epilepsy with and without hippocampal sclerosis at 7T. J Magn Reson Imaging 2017;45(5):1359–70.
[19] Bernhardt BC, Bernasconi A, Liu M, Hong SJ, Caldairou B, Goubran M, et al. The spectrum of structural and functional imaging abnormalities in temporal lobe epilepsy. Ann Neurol 2016;80(1):142–53.
[20] Bernhardt BC, Fadaie F, Liu M, et al. Temporal lobe epilepsy: hippocampal pathology modulates connectome topology and controllability. Neurology 2019;92(19):e2209–20.
[21] Engel J. A proposed diagnostic scheme for people with epileptic seizures and with epilepsy: report of the ILAE Task Force on Classification and Terminology. Epilepsia 2001;42(6):796–803.
[22] Li W, Jiang Y, Qin Y, Zhou B, Lei D, Luo C, et al. Dynamic gray matter and intrinsic activity changes after epilepsy surgery. Acta Neurol Scand 2021;143(3):261–70.
[23] Fischl B. FreeSurfer. Neuroimage 2012;62(2):774–81.
[24] Riederer F, Seiger R, Lanzenberger R, et al. Automated volumetry of hippocampal subfields in temporal lobe epilepsy. Epilepsy Res 2021;175:106692.
[25] Li W, An D, Tong X, Liu W, Xiao F, Ren J, et al. Different patterns of white matter changes after successful surgery of mesial temporal lobe epilepsy. Neuroimage Clin 2019;21:101631.
[26] Jenkinson M, Beckmann CF, Behrens TE, Woolrich MW, Smith SM. FSL. Neuroimage 2012;62(2):782–90.
[27] Smith SM, Jenkinson M, Johansen-Berg H, Rueckert D, Nichols TE, Mackay CE, et al. Tract-based spatial statistics: voxelwise analysis of multi-subject diffusion data. Neuroimage 2006;31(4):1487–505.
[28] Hua K, Zhang J, Wakana S, Jiang H, Li X, Reich DS, et al. Tract probability maps in stereotaxic spaces: analyses of white matter anatomy and tract-specific quantification. Neuroimage 2008;39(1):336–47.
[29] Xue K, Luo C, Zhang D, Yang T, Li J, Gong D, et al. Diffusion tensor tractography reveals disrupted structural connectivity in childhood absence epilepsy. Epilepsy Res 2014;108(1):125–38.
[30] Tzourio-Mazoyer N, Landeau B, Papathanassiou D, Crivello F, Etard O, Delcroix N, et al. Automated anatomical labeling of activations in SPM using a macroscopic anatomical parcellation of the MNI MRI single-subject brain. Neuroimage 2002;15(1):273–89.
[31] Rubinov M, Sporns O. Complex network measures of brain connectivity: uses and interpretations. Neuroimage 2010;52(3):1059–69.
[32] Boccara CN, Sargolini F, Thoresen VH, Solstad T, Witter MP, Moser EI, et al. Grid cells in pre- and parasubiculum. Nat Neurosci 2010;13(8):987–94.
[33] Sullenberger T, Don H, Kumar SS. Functional connectivity of the parasubiculum and its role in temporal lobe epilepsy. Neuroscience 2019;410:217–38.
[34] van Vliet EA, Aronica E, Tolner EA, Lopes da Silva FH, Gorter JA. Progression of temporal lobe epilepsy in the rat is associated with immunocytochemical changes in inhibitory interneurons in specific regions of the hippocampal formation. Exp Neurol 2004;187(2):367–79.
[35] Cardoso A, Lukoyanova EA, Madeira MD, Lukoyanov NV. Seizure-induced structural and functional changes in the rat hippocampal formation: comparison between brief seizures and status epilepticus. Behav Brain Res 2011;225(2):538–46.
[36] Boido D, Jesuthasan N, de Curtis M, Uva L. Network dynamics during the progression of seizure-like events in the hippocampal-parahippocampal regions. Cereb Cortex 2014;24(1):163–73.
[37] Concha L, Beaulieu C, Collins DL, Gross DW. White-matter diffusion abnormalities in temporal-lobe epilepsy with and without mesial temporal sclerosis. J Neurol Neurosurg Psychiatry 2009;80(3):312–9.
[38] Romanowski CA, Hutton M, Rowe J, Yianni J, Warren D, Bigley J, et al. The anatomy of the medial lemniscus within the brainstem demonstrated at 3 Tesla with high resolution fat suppressed T1-weighted images and diffusion tensor imaging. Neuroradiol J 2011;24(2):171–6.

[39] Chiang S, Haneef Z. Graph theory findings in the pathophysiology of temporal lobe epilepsy. Clin Neurophysiol 2014;125(7):1295–305.
[40] Latora V, Marchiori M. Efficient behavior of small-world networks. Phys Rev Lett 2001;87(19):198701.
[41] Vaessen MJ, Jansen JF, Vlooswijk MC, Hofman PA, Majoie HJ, Aldenkamp AP, et al. White matter network abnormalities are associated with cognitive decline in chronic epilepsy. Cereb Cortex 2012;22(9):2139–47.